International Journal on Advanced Science Engineering Information Technology

Vol.15 (2025) No. 1
ISSN: 2088-5334

Computational Investigation on the Fatigue Behavior of Titanium Alloy Ti-6Al-2Sn-4Zr-2Mo under Dynamic Loads by Consideration of Ambient Temperature

Ali Talib Shomran [a], Haideer Talib Shomran [b], Emad Kamil Hussein [c], Hussein Kadhim Sharaf [d,e,*], Thiago Santos [f], Caroliny Santos [f]

[a] *Mechanical Equipment and Machines Department, Mussaib Technical College, Al Furat Al Awsat Technical University, Babil, Iraq*
[b] *Water Resources Department, Al-Mussaib Technical Institute, Al-Furat Al-Awsat Technical University, Babylon, Babil, Iraq*
[c] *Prosthetics and Orthotics Department, Mussaib Technical College, Al Furat Al Awsat Technical University, Babil, Iraq*
[d] *AL-Muqdad College of Education, University of diyala, Diyala, Iraq*
[e] *University of Bilad al rafidain, Baquba, Diyala Governorate, Iraq*
[f] *Technology center, Federal University of Rio Grande do Norte, Av. Prof. Sen. Salgado Filho, Natal, Rio Grande do Norte, Brazil*

*Corresponding author: *hk.sharaf92@gmail.com*

***Abstract*—In this study, a static structural tool in ANSYS software was utilized in order to carry out a numerical evaluation of the fatigue behavior of titanium alloy Ti-6Al-2Sn-4Zr-2Mo when subjected to dynamic loads. A static structure was utilized in the process of performing the analysis and meshing it using the Ansys program. A load of 3.15 (KN) has been assumed to be applied to the plate, and it is applied in the opposite direction of the plate. When it comes to the tiredness phase, the GOODMAN criteria have been utilized. Using grid independent testing, the outcomes that were initiated have been validated. The 3.15 KN of loads that were applied have been accounted for as the cause of the total deformation. There is a height of 7.0e-7 meters. For the applied load of 9.5E5 cycles, the information on life due practice has been proven and reached. Based on the plied load that was placed on the alloy, the equivalent stress estimated has been determined. The eq. stress reached a maximum value of 6.2E6 Pa at its highest point.**

Keywords—Dynamics loads; fatigue behavior; titanium alloy; FEM; static structure.

Manuscript received 15 Sep. 2024; revised 29 Nov. 2024; accepted 5 Jan. 2025. Date of publication 28 Feb. 2025.
IJASEIT is licensed under a Creative Commons Attribution-Share Alike 4.0 International License.

I. INTRODUCTION

The AM process is now state-of-the-art for making metal parts with intricate geometries [1]. Amplified manufacturing has a bright future because to three key reasons: increased output, credibility, and geometrical freedom. A wide variety of materials can be used to construct the buildings. Materials like titanium, stainless steel, alloys based on nickel, and aluminum have mechanical qualities that can be used in many different ways [2]. Constructing a three-dimensional geometric model begins with layering [3]. As a result, AM offers several benefits over traditional processing methods, including prototyping, quick manufacturing, material efficiency, and product customization. However, residual stress, process-induced flaws, and material anisotropy are all outcomes of layer-wise fabrication. One of the main drawbacks of AM is the unfavorable impact it has on the mechanical behavior of the finished product. This results in components of inferior quality when compared to those manufactured using more conventional methods [4].

Microstructure variations are caused by the quick solidification that occurs because of the high-temperature gradients that occur during the AM process. The material also experiences residual strains due to heat gradients. Due to the solidification process, the sample shrinks; nonetheless, the residual stresses can undergo a transformation from tensile to compressive, or inversely, depending on the additional layer that is "printed" on top. Another effect of the fast and frequent heating and cooling process employed in layer-by-layer fabrication is variations in residual stresses, with larger stresses in the scanning direction [5]. These values often dictate the material's fatigue resistance.

Researchers looked at how different scanning setups and procedures affected the microstructure and pore initiations in Selective Laser Melting (SLM) AM in their study [6]. Fatigue performance was comparable to that of the wrought sample after post-built annealing treatments reduced microstructure anisotropy and practically eliminated residual stresses [7]. Fatigue life was significantly affected by the shrinkage of sample pores caused by the HIP process; cracks started at procedure-induced defects. Anisotropy was discovered in the SLM-made FCGR of Ti6Al4V in yet another research by [8]. Here, the FCGR felt the effects of extraordinarily high compressive pressures caused by the building's directional movement. The samples with the weakest fracture toughness tend to exhibit residual stresses that are predominantly tensile. Residual stress distributions with core compressive stresses and margin tension were seen in the as-built samples, in line with previous research on AM material outcomes [9]. Research by [10] into the relationship between residual stress and fatigue crack growth rate (FCGR) revealed that the behavior of fatigue cracks had a significant impact on residual stresses.

When studying Ti6Al4V samples made by SLM, every research revealed that the largest residual stresses ran perpendicular to the scan direction. Research has highlighted post-built annealing treatments to reduce anisotropy of mechanical properties and alleviate these stresses [11]. Although a lot of experimental work was done to understand what causes stresses in, various studies have been conducted to quantify the samples' stresses and places. The remaining stresses were predicted using a two-dimensional finite element thermomechanical model that contains a moving heat source, developed by [12]. Furthermore, the effects of AM process parameters on residual stress distributions were investigated by [13,14] using 3D models. These parameters included layer thickness and heat input. Another study [15] further investigated the residual stress distributions produced by different laser scan techniques using linked FE models.

For conducting fatigue crack growth testing, two types of Compact Tension (C(T)) samples were produced utilizing AM in the published research. On one type of platform, SLM specimens were built one by one; on the other, a continuous extended block was used to slice individual specimens [16]. After the notch was made, the samples were machined to make them smooth, following ASTM standard E647 [17]. The impact of surface and notch machining on residual stress was highlighted by [18] in their examination of C(T) sample production. To start, the as-built samples had twice as high longitudinal tensile strains around the sample's edges as they did in the middle, where longitudinal compressive stresses were exceptionally high. Secondly, following surface machining, the sample shrank slightly, which reduced compressive stresses in the Centre by 55% and tensile tensions at the sample's edges by a similar amount.

Finally, the notch machining redirected residual stress and decreased tensile stress. Although the machining process significantly affected the stress release, stresses, which comprised both tensile and compressive strains, varied across the samples' lengths. However, because of the heat treatment, the stresses in the samples were either eliminated or kept at low levels throughout. Fatigue testing conducted on SLM C(T) samples revealed increased residual stresses and accelerated crack propagation. According to previous research [19] that demonstrated a comparable result in fatigue propagation testing, isotropy affects the samples' fatigue characteristics.

When it comes to creating metal components with complex shapes, the AM method is now at the cutting edge [20]. Due to its geometrical flexibility, productivity, and durability, AM holds a lot of promises. The industries that utilize them are determined by their mechanical properties.

Layer construction is the initial stage in the fabrication of three-dimensional geometric designs [21]. As a result, AM offers several benefits over traditional processing methods, including prototyping, quick manufacturing, material efficiency, and product customization. However, residual stress, process-induced flaws, and material anisotropy are all outcomes of layer-wise fabrication. One of the main drawbacks of AM is the unfavorable impact it has on the mechanical behavior of the finished product. Components made using this approach are of lower quality compared to those made using more traditional methods [22].

Rapid solidification due to high-temperature gradients in the AM process is the root cause of microstructure differences. Because of thermal gradients, the material also undergoes residual strains. The sample gets smaller as it solidifies, but the residual stresses can change from tensile to compressive or vice versa, depending on the extra layer that's "printed" on top. Because layer-by-layer production involves rapid and repeated heating and cooling, residual stress also varies, with greater stresses along the scanning direction [23]. Material fatigue resistance is often dictated by these values.

In relation to different scanning processes and parameters, the microstructure and pore initiations in Selective Laser Melting (SLM) AM were examined in [24]. The fatigue life of the sample has been decreased because the pores shrank during the HIP process. Procedural errors were the initial points of failure. Ti6Al4V FCGRs produced by SLM showed isotropy, according to yet another research. Extremely strong compressive stresses, brought on by the building's directional shift, were felt by the FCGR here. Tensile residual stresses are more common in samples with low fracture toughness. The as-built samples showed residual stress distributions with core compressive stresses and margin tension, which is consistent with other studies on the results of AM materials [25].

The behavior of fatigue cracks significantly affected residual stresses, according to research [26] that examined the relationship between residual stresses and fatigue crack growth rate (FCGR). The biggest residual stresses ran perpendicular to the scan direction while investigating Ti6Al4V samples created by SLM, according to the investigations. Anisotropy in mechanical characteristics can be reduced, and these stresses can be alleviated using post-built annealing treatments, according to research [27]. The sources of residual stresses in SLM have been the subject of much experimental investigation, but numerical studies have been used to measure the stresses in various alloys . A two-dimensional finite element thermomechanical model with a moving heat source was created by [28]. Authors of [29] examined how different AM process parameters affected the distribution of residual stresses. Among these factors were the heat input and layer thickness. Using coupled 3D thermo-mechanical FE models, another research [30] dug more into the residual stress distributions generated by various laser scan methods. The samples were machined to make them smooth after the notch was formed, following ASTM standard E647 [35]. In this study, Computational Investigation on the Fatigue Behavior of Titanium Alloy Ti-6Al-2Sn-4Zr-2Mo under Dynamic Loads

II. Materials and Method

A. Characteristics of the Titanium Alloy Ti-6Al-2Sn-4Zr-2Mo

To begin the process of determining the fatigue behavior of the titanium alloy Ti-6Al-2Sn-4Zr-2Mo, the first step of the approach involves the specification of engineering data. This is necessary in order to carry out the procedure. For the procedure to be carried out successfully, this is a prerequisite. This is something that absolutely needs to be done in order to successfully carry out the simulation. Poisson's ratio is 0.33, and the engineering in modulus of elasticity E = 110 GPa is the required number of features for the sum. These are the characteristics that are important to possess. All of these characteristics are required in order to successfully complete the summary. The simulation process cannot be finished without the existence of a density, which is the second essential component that must be present in order for the simulation to be taken into consideration. After conducting the necessary calculations, it has been established that the titanium alloy Ti-6Al-2Sn-4Zr-2Mo has a density of 4, 539.50 kilograms per cubic metre (kg/m3).

B. Boundary conditions

By use the Static Structure tool in combination with the fatigue tool that was introduced into the ANSYS software development environment, Goodman's theory was employed in order to calculate fatigue. This was accomplished by utilizing the Static stricter tool. The load has been applied to the plate in a symmetrical way, and the total value of the loads that have been applied up to this point has amounted to 3.15 kilonewtons respectively.

C. Physical geometry and mesh

A model of the geometry of the current investigation was developed with the assistance of the software application known as AutoCAD. After that, the model was transferred to the SpaceCalim program so that it could be subjected to further examination. A component of the ansys simulation program, the static tool, was utilized in order to successfully manufacture the mesh model of the titanium alloy. This was done by the utilization of the software. There are 23000 nodes and 21020 components in the modelled shape, according to the statical calculation of the mesh, which provides this information. In order to obtain this information, the models were utilized. As can be seen in Figure 1, it was necessary to generate the unstructured shape of the parts in order to accommodate the intricacy of the geometry. To accommodate the geometry, something was done in order to accommodate it. Hexahedral element meshing types were employed in order to achieve the goal of producing outcomes that were more precise.

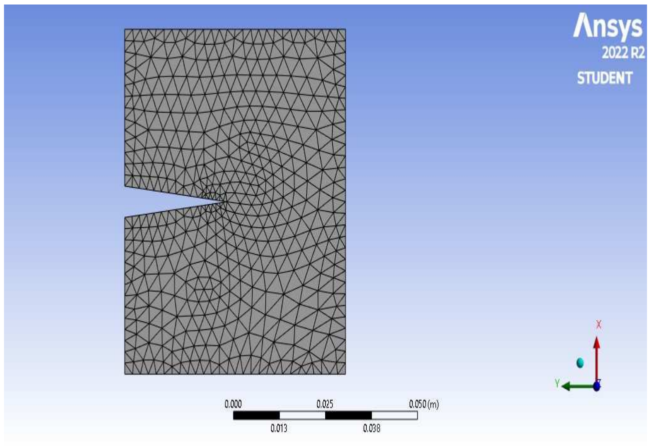

Fig. 1 The meshed model

III. Results and Discussion

A. Investigation-based total deformation

A load of 3.15 kilonewtons was applied to the alloy plate in two different orientations while the height stayed the same. This was done in order to achieve the goals that were set for this experiment. In the course of the application of this load, the greatest amount of deformation that took place was 7.0e-7 meters. Figure 3, which is a graphical representation of the data, shows the precise location of the deformation that is the most significant. When the fractures first appear, it is possible to observe the concertation of the deformation at this stage. This occurs at the beginning of the fractures in the bone formation.

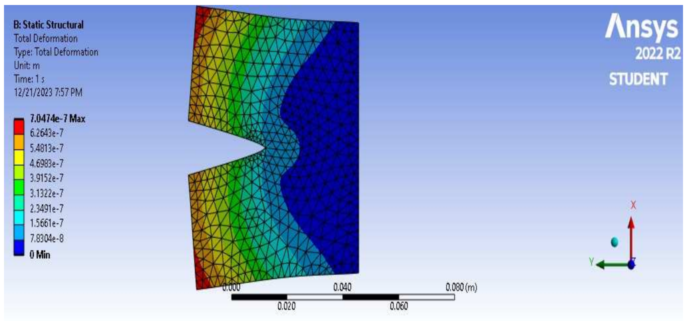

Fig. 2 Total deformation

According to the conclusions of the numerical analysis, the maximum reach deformation is 7.0e-7 meters, and the force that causes it is 3.15 kilonewtons. When the force is applied in both directions at its lowest attainable level, which is 2.15 kilonewtons, there is minimum deformation that takes place. In the conclusions of the numerical analysis, it was discovered that there exist linear connections between the components that were subject to investigation. A static structure tool was utilized in order to do the deformation calculation. This was accomplished with the assistance of the ANSYS program. Figure 3 illustrates the linear relationship that exists between the deformation that occurs on the plate that is made of alloy as a consequence of the dynamical load that is given to the plate. There is a direct correlation between the two.

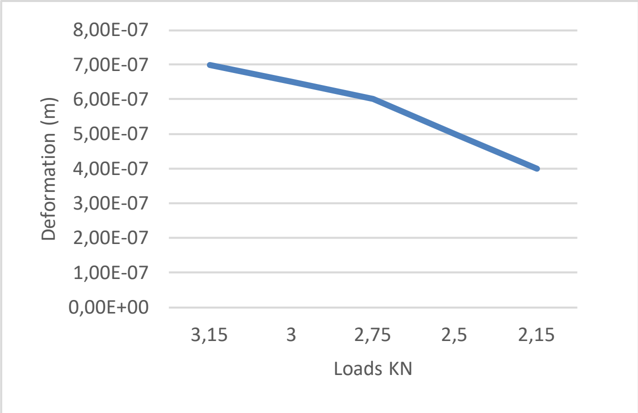

Fig. 3 Deflections due to applied dynamic load

B. *Lifetime Analysis of the Titanium Alloy Ti-6Al-2Sn-4Zr-2Mo*

An inquiry into the lifetime study of the titanium alloy Ti-6Al-2Sn-4Zr-2Mo was carried out with the assistance of the Static structural tool that is included in the ANSYS program. The fatigue tool served as a source of information for this inquiry. It was determined that a load of 3.15 kilonewtons was applied to both sides of the plate for the purpose of the current numerical study. Figure 4 illustrates the lifetime of the titanium alloy represented by the formula Ti-6Al-2Sn-4Zr-2Mo. A varied range of dynamic loads is used to measure its lifespan, and the results are shown here. It has been determined that the maximum lifespan has been accomplished with only a little amount of load being applied. It is possible to draw the conclusion that the connection between the variables (Loads and Lifetime) is linear, based on the inferences that can be drawn according to the numerical data. For the potential load of 3.15 kilonewtons, it has been established that the lifespan has reached a total of 6 times 10 to the power of six cycles.

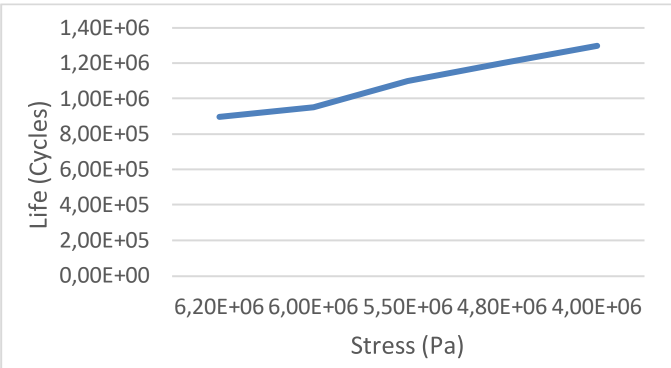

Fig. 4 Lifetime analysis

C. *Equivalent Stress on the plate of titanium alloy Ti-6Al-2Sn-4Zr-2Mo*

An investigation was carried out with the assistance of the Static structural tool that is a component of the ANSYS software in order to examine the Equivalent Stress on the Plate of the titanium alloy Ti-6Al-2Sn-4Zr-2Mo. This process was carried out in order to explore Equivalent Stress. The numerical analysis that is displayed in the image makes it abundantly evident that the location where the majority of the focus is located is the sharp corner, which is also referred to as the root. This is the region that is the primary focus. For the purpose of carrying out these observations, the static tools that are included in the Ansys program were employed. In addition, the application includes some features for your use. Based on the results of the calculations that were carried out, it was established that the loads that were simultaneously applied to both sides of the plate amounted to 3.25 kilonewtons. The results of numerical research are depicted in Figure 5, which includes the data that the maximum consequences of alternative stress reached 6.2E6 Pa. Utilization of the system led to the discovery of this information.

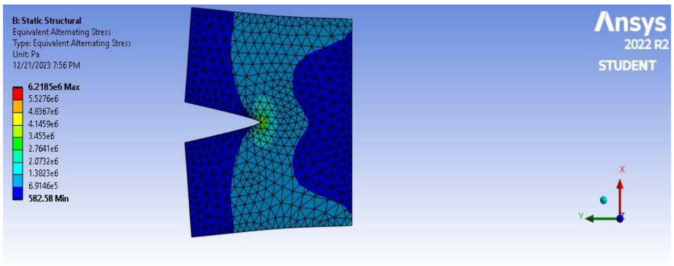

Fig. 5 Equivalent Stress analysis

Figure 6 provides a visual representation of the connection that exists between the alternative stress and the loads that are applied to the titanium alloy. Through the use of the fatigue tool in conjunction with the statistical tool that is a part of the Antsy software, a numerical representation of the stress has been developed. The numerical findings revealed that the maximum stress reached 6.2E Pa when the applied weights were 3.15 Kn. This was established based on the outcomes of the experiments. When the applied loads were at their lowest value, which was 2.5KN, the minimum stress reached 4.9e6 Pa. This was the case when the applied loads were at their lowest value. In conclusion, the data showed that there is a linear relationship between the stress and the load that was introduced into the system.

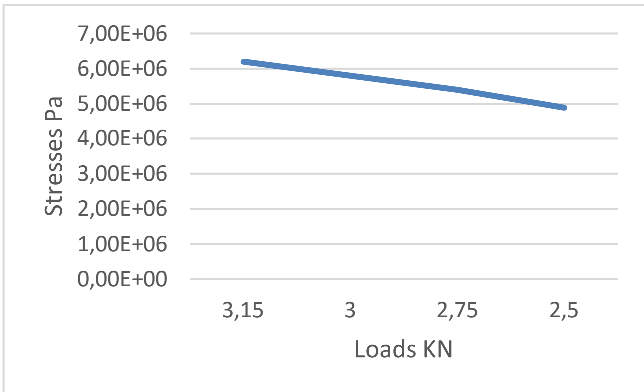

Fig. 6 Alternative stress with applied loads

D. *Investigation of Biaxiality indication*

Regarding the information that is essential, it is described as the stress that is of a lesser value divided by the stress that is of a greater magnitude. In the current investigation, the Biaxiality indication is 0.88, which is close to the value of 1, when 3.15 kilonewtons are applied. This indicates that the load is the linear load, as demonstrated in Figure 7.

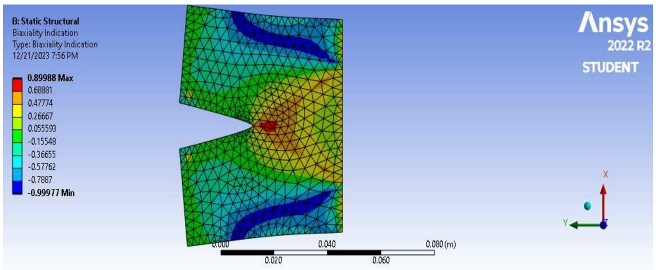

Fig. 7 Biaxiality indication

IV. CONCLUSION

The conclusion is that a static structural tool inside the ANSYS was utilized in order to carry out a numerical evaluation of the fatigue behavior of titanium alloy Ti-6Al-2Sn-4Zr-2Mo when it was subjected to dynamic loads. For the purpose of carrying out the analysis and meshing it with the help of the Ansys tool, a static structure was utilized. It is assumed that a force of 3.15 kilonewtons (KN) is being applied to the plate, and this weight is being applied in the opposite direction of the plate. The parameters established by the GOODMAN framework have been applied to the fatigue phase of the process. The outcomes that were launched have been validated through the utilization of grid independent testing, which was accomplished. Taking into consideration the 3.15 kilonewtons of loads that were applied, it has been determined that the complete deformation was caused by those loads. It is seven and a half meters. It has been proved and accomplished that the information on life due practice has been reached for the imposed load of 9.5E5 cycles. The estimated equivalent stress has been obtained by using the plied load that was applied to the alloy as the foundation for the calculation. The equation stress reached its highest point at 6.2E6 Pa, which was the maximum value it could reach.

ACKNOWLEDGMENT

No grant did not fund this research.

REFERENCES

[1] D. Suárez Fernández, B. P. Wynne, P. Crawforth, K. Fox, and M. Jackson, "The effect of forging texture and machining parameters on the fatigue performance of titanium alloy disc components," *International Journal of Fatigue*, vol. 142, p. 105949, Jan. 2021, doi:10.1016/j.ijfatigue.2020.105949.

[2] D. Ballat-Durand, S. Bouvier, M. Risbet, and W. Pantleon, "Through analysis of the microstructure changes during linear friction welding of the near-α titanium alloy Ti-6Al-2Sn-4Zr-2Mo (Ti6242) towards microstructure optimization," *Materials Characterization*, vol. 151, pp. 38–52, May 2019, doi: 10.1016/j.matchar.2019.02.027.

[3] Z. Guo et al., "Linear friction welding of Ti60 near-α titanium alloy: Investigating phase transformations and dynamic recrystallization mechanisms," *Materials Characterization*, vol. 194, p. 112424, Dec. 2022, doi: 10.1016/j.matchar.2022.112424.

[4] S. Hémery, P. Villechaise, and D. Banerjee, "Microplasticity at Room Temperature in α/β Titanium Alloys," *Metallurgical and Materials Transactions A*, vol. 51, no. 10, pp. 4931–4969, Aug. 2020, doi:10.1007/s11661-020-05945-4.

[5] T. Tsuru, M. Itakura, M. Yamaguchi, C. Watanabe, and H. Miura, "Dislocation core structure and motion in pure titanium and titanium alloys: A first-principles study," *Computational Materials Science*, vol. 203, p. 111081, Feb. 2022, doi:10.1016/j.commatsci.2021.111081.

[6] R. Zhang, Q. Zhao, Y. Zhao, D. Guo, and Y. Du, "Research Progress on Slip Behavior of α-Ti under Quasi-Static Loading: A Review," *Metals*, vol. 12, no. 10, p. 1571, Sep. 2022, doi: 10.3390/met12101571.

[7] N. H. A. Alyaseri et al., "Exploring the modeling of socio-technical systems in the fields of sport, engineering, and economics," *Rev. Iberoam. Psicol. Ejerc. Deporte*, vol. 18, no. 3, pp. 338–341, 2023.

[8] K. A. Kurmoiartseva, N. A. Knyazev, N. V. Kotelnikova, and P. V. Trusov, "Viscoelastoplastic model of titanium alloys with the influence of pile-up dislocation on the crack nucleation," *Physical Mesomechanics of Condensed Matter: Physical Principles of Multiscale Structure Formation and the Mechanisms of Nonlinear Behavior: MESO2022*, vol. 2899, p. 020084, 2023, doi:10.1063/5.0163227.

[9] L. T. Mouhmmd, M. A. Rahima, A. M. Mohammed, H. F. Hasan, A. S. Alwan, and H. K. Sharaf, "The effect of firm type on the relationship between accounting quality and trade credit in listed firms," *Corporate and Business Strategy Review*, vol. 4, no. 2, pp. 175–183, 2023, doi: 10.22495/cbsrv4i2art16.

[10] F. Jin et al., "Heat-pattern induced non-uniform radial microstructure and properties of Ti-6Al-4V joint prepared by rotary friction welding," *Materials Characterization*, vol. 195, p. 112536, Jan. 2023, doi:10.1016/j.matchar.2022.112536.

[11] I. O. B. Al-Fahad, H. kadhim Sharaf, L. N. Bachache, and N. K. Bachache, "Identifying the mechanism of the fatigue behavior of the composite shaft subjected to variable load," *Eastern-European Journal of Enterprise Technologies*, vol. 3, no. 7 (123), pp. 37–44, Jun. 2023, doi: 10.15587/1729-4061.2023.283078.

[12] M. Lin, Y. Liu, C. Oskay, and X. Zhang, "Microstructure-Informed Reduced-Order Modeling of Fatigue Initiation in a Titanium Skin Panel Subjected to Thermo-Mechanical Loading," *AIAA SCITECH 2022 Forum*, Jan. 2022, doi: 10.2514/6.2022-0210.

[13] V. Anil Kumar, R. K. Gupta, M. J. N. V. Prasad, and S. V. S. Narayana Murty, "Recent advances in processing of titanium alloys and titanium aluminides for space applications: A review," *Journal of Materials Research*, vol. 36, no. 3, pp. 689–716, Jan. 2021, doi: 10.1557/s43578-021-00104-w.

[14] M. A. Marir, E. L. Sheng, I. O. Bachi, and M. R. Isa, "Tensile efficiency and fatigue life of similar and dissimilar carbon steel joints subjected to rotary friction welding," *Journal of Advanced Joining Processes*, vol. 8, p. 100168, Nov. 2023, doi:10.1016/j.jajp.2023.100168.

[15] M. A. Marir, E. L. Sheng, M. R. Isa, and I. O. Bachi, "Destructive and nondestructive remaining fatigue life prediction methods of metals: a review," *Journal of Mechanical Science and Technology*, vol. 37, no. 8, pp. 3999–4015, Aug. 2023, doi: 10.1007/s12206-023-0716-y.

[16] S. Rajan, P. Wanjara, J. Gholipour, and A. S. Kabir, "Fatigue Behavior of Linear Friction Welded Ti-6Al-4V and Ti-6Al-2Sn-4Zr-2Mo-0.1Si Dissimilar Welds," *Materials*, vol. 14, no. 11, p. 3136, Jun. 2021, doi:10.3390/ma14113136.

[17] B. Sefer, R. Gaddam, J. J. Roa, A. Mateo, M.-L. Antti, and R. Pederson, "Chemical milling effect on the low cycle fatigue properties of cast Ti–6Al–2Sn–4Zr–2Mo alloy," *International Journal of Fatigue*, vol. 92, pp. 193–202, Nov. 2016, doi:10.1016/j.ijfatigue.2016.07.003.

[18] A. Alrawi, "Feasibility Study of a Project Performance-The Validation of Measurements," *2020 2nd Annual International Conference on Information and Sciences (AiCIS)*, pp. 178–182, Nov. 2020, doi:10.1109/aicis51645.2020.00037.

[19] I. O. B. Al-Fahad, A. D. Hassan, B. M. Faisal, and H. kadhim Sharaf, "Identification of regularities in the behavior of a glass fiber-reinforced polyester composite of the impact test based on ASTM D256 standard," *Eastern-European Journal of Enterprise Technologies*, vol. 4, no. 7 (124), pp. 63–71, Aug. 2023, doi:10.15587/1729-4061.2023.286541.

[20] R. Bandyopadhyay, A. W. Mello, K. Kapoor, M. P. Reinhold, T. F. Broderick, and M. D. Sangid, "On the crack initiation and heterogeneous deformation of Ti-6Al-4V during high cycle fatigue at high R ratios," *Journal of the Mechanics and Physics of Solids*, vol. 129, pp. 61–82, Aug. 2019, doi: 10.1016/j.jmps.2019.04.017.

[21] P. Ouyang, X. Luo, Z. Dong, and S. Zhang, "Numerical Prediction of the Effect of Laser Shock Peening on Residual Stress and Fatigue Life of Ti-6Al-4V Titanium Alloy," *Materials*, vol. 15, no. 16, p. 5503, Aug. 2022, doi: 10.3390/ma15165503.

[22] S. A. S. Almtori, I. O. B. Al-Fahad, A. H. Taha Al-temimi, and A. K. Jassim, "Characterization of polymer based composite using neuro-fuzzy model," *Materials Today: Proceedings*, vol. 42, pp. 1934–1940, 2021, doi: 10.1016/j.matpr.2020.12.238.

[23] O. Lypchanskyi et al., "The analysis of flow behavior of Ti-6Al-2Sn-4Zr-6Mo alloy based on the processing maps*," International Journal of Material Forming*, vol. 14, no. 4, pp. 523–532, Jan. 2020, doi:10.1007/s12289-019-01533-z.

[24] M. Roshani, H. R. Abedi, and A. Saboori, “Comparing the Cold, Warm, and Hot Deformation Flow Behavior of Selective Laser-Melted and Electron-Beam-Melted Ti–6Al–2Sn–4Zr–2Mo Alloy,” *Advanced Engineering Materials*, vol. 26, no. 2, Nov. 2023, doi:10.1002/adem.202301046.

[25] S. Rajan, P. Wanjara, J. Gholipour, and A. S. Kabir, “Joining of Dissimilar Alloys Ti-6Al-4V and Ti-6Al-2Sn-4Zr-2Mo-0.1Si Using Linear Friction Welding,” *Materials*, vol. 13, no. 17, p. 3664, Aug. 2020, doi: 10.3390/ma13173664.

[26] R. F. Ghazi, J. S. Chiad, and F. M. Abdulghani, “Design and manufacturing a smart shoe for diabetic foot ulcer monitoring and prediction system using internet-of-things technology,” *Journal of the Brazilian Society of Mechanical Sciences and Engineering*, vol. 46, no. 2, Jan. 2024, doi: 10.1007/s40430-023-04591-2.

[27] F. T. Al-Maliky and J. S. Chiad, “Study and analysis the flexion moment in active and passive knee prosthesis using back propagation neural network predictive,” Journal of the Brazilian Society of Mechanical Sciences and Engineering, vol. 44, no. 11, Oct. 2022, doi:10.1007/s40430-022-03850-y.

[28] M. M. Yahya, A. M. Al-Mushehdany, and H. J. M. Alalkawi, “Evaluation of Buckling of 2024-T3 under High Temperatures,” *International Journal of Heat and Technology*, vol. 40, no. 4, pp. 947–952, Aug. 2022, doi: 10.18280/ijht.400411.

[29] A. AL-Mushehdany, M. M. Yahya, E. K. Ibrahim, and H. J. M. Alalkawi, “Nano reinforcement technique as a tool for enhancement the mechanical and fatigue properties,” *Curved and Layered Structures*, vol. 9, no. 1, pp. 345–351, Jan. 2022, doi: 10.1515/cls-2022-0026.

[30] B. M. Faisal et al., “Finite Element Analysis for Aluminium Alloy 7075-T6 Subjected to the Bending-Torsional Variable Phase of Fatigue Loading,” *Journal of Advanced Research in Applied Mechanics*, vol. 128, no. 1, pp. 62–71, Nov. 2024, doi:10.37934/aram.128.1.6271.